

Northward extension of intense monsoonal activity into the southwestern United States

Jeremy E. Diem

Department of Anthropology and Geography, Georgia State University, Atlanta, Georgia, USA

Received 3 March 2005; revised 9 June 2005; accepted 20 June 2005; published 19 July 2005.

[1] Although it is centered in northwestern Mexico, the Mexican monsoon also has been shown to impact portions of the southwestern United States. To provide more information about the spatial distribution of monsoonal impacts in the Southwest, this study employed multiple linear regression modeling to reduce local topographic impacts on monsoonal precipitation to reveal intense monsoonal activity within the Gila River basin. The precipitation data were daily precipitation totals from 115 stations from June 16–September 15 of 1996–2002. An intense monsoonal zone was found in the south-central portion of the basin. Therefore, intense monsoonal activity associated with the Sierra Madre Occidental in northwestern Mexico extended into south-central and southeastern Arizona but not into New Mexico. **Citation:** Diem, J. E. (2005), Northward extension of intense monsoonal activity into the southwestern United States, *Geophys. Res. Lett.*, *32*, L14702, doi:10.1029/2005GL022873.

1. Introduction

[2] The Mexican monsoon causes much of northwestern Mexico and parts of the southwestern United States to receive over 60% of annual precipitation during the June–September period [e.g., *Douglas et al.*, 1993]. The monsoon is most intense over the Sierra Madre Occidental (SMO), which is located east of the Gulf of California in western Mexico; this area receives over 400 mm of precipitation from June through September [*Higgins et al.*, 1999]. Further, there is mounting evidence [e.g., *Douglas et al.*, 1993; *Stensrud et al.*, 1995; *Berbery*, 2001; *Wright et al.*, 2001; *Mitchell et al.*, 2002; *Saleeby and Cotton*, 2004] that the eastern tropical Pacific Ocean and the Gulf of California, rather than the Gulf of Mexico, supply a majority of the moisture that fuels monsoonal storms.

[3] The exact geographic extent of the Mexican monsoon is difficult to determine. The monsoon region, however, can be partitioned into a core and periphery [see *Douglas et al.*, 1993]. The intensity of the monsoon decreases with an increase in latitude, with an abrupt decrease in precipitation occurring from $\sim 30^{\circ}\text{N}$ to $\sim 32^{\circ}\text{N}$, which is at the northern edge of the SMO and includes southern Arizona and southwestern New Mexico [*Higgins et al.*, 1999]. Based on results given by *Comrie and Glenn* [1998] and *Higgins et al.* [1999], July–August precipitation totals in this region are about one-third to one-half the totals in the SMO region. Therefore, the monsoon is relatively weak in the peripheral region.

[4] Topography, especially elevation, exerts a major influence on spatial variations in monsoonal activity in the peripheral region. *Michaud et al.* [1995] used elevation data alone to reduce topographic effects on precipitation totals throughout Arizona and New Mexico. *Comrie and Broyles* [2002] and *Skirvin et al.* [2003] reported elevation to be an important control of precipitation in southern Arizona. Although the above studies did confirm the importance of topography as a precipitation control, none of the studies removed the influence of multiple topographic factors to show the northward advancement of the Mexican monsoon.

[5] In order to improve the understanding of the geographic extent of the Mexican monsoon, the purpose of this paper is to reveal intense monsoonal activity within the Gila River basin by minimizing local topographic controls. The Gila River basin, which encompasses most of the southern half of Arizona and part of western New Mexico (Figure 1), is an excellent study domain because sub-monthly precipitation totals have been measured at over 300 weather stations in the basin during the past decade.

2. Data

[6] The principal dataset consisted of daily precipitation totals measured at Automated Local Evaluation in Real Time (ALERT), Arizona Meteorological Network (AZMET), and National Weather Service (NWS) stations from June 16–September 15 of 1996–2002. The 92-day period from mid-June to mid-September was chosen because the thermal-low system – which is a main feature of the monsoonal circulation – is typically over the desert region during that time period [*Rowson and Colucci*, 1992]. Hourly precipitation totals were obtained for both the ALERT and AZMET stations from the Flood Control District of Maricopa County and The University of Arizona Cooperative Extension, respectively. Daily precipitation totals were obtained for the NWS stations from the National Oceanic and Atmospheric Administration.

[7] Since most of the NWS stations had morning observation times (i.e. 7 A.M. or 8 A.M.), the hourly totals at the ALERT and AZMET stations were aggregated to daily totals comprising the 24-hour period beginning and ending at 8 A.M. Daily precipitation totals were associated with the day on which most of the precipitation probably occurred. Since monsoonal activity (i.e. lightning and precipitation) typically peaks in the evening [*Balling and Brazel*, 1987; *Watson et al.*, 1994], precipitation totals for all morning-observation stations and most afternoon-observation stations were moved to the previous day. For the ALERT and AZMET stations, only those days having 18 or more hours with valid data were given valid precipitation totals.

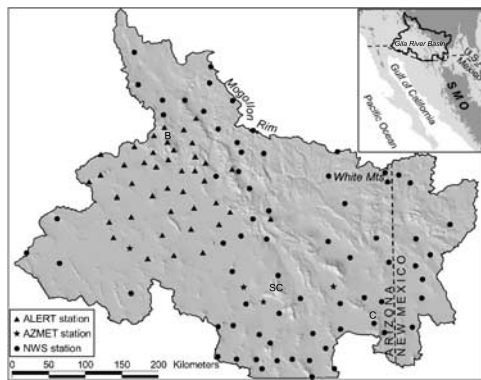


Figure 1. Weather stations in and topography of the Gila River basin. Also shown is the basin's location in the southwestern United States and its proximity to the Sierra Madre Occidental (SMO). Darker areas in the upper map are greater than or equal to 1,500 m above sea level. Locations of the Bradshaw Mountains (B), Chiricahua Mountains (C), and Santa Catalina Mountains (SC) are indicated on the lower map.

Daily precipitation totals were upwardly adjusted using the $24/x$ ratio, where x is the number of hours with valid data.

[8] Precipitation totals at ALERT stations – which employed tipping-bucket rain gauges – were almost always lower than totals at approximately co-located NWS stations that employed standard rain gauges. For nine pairs of stations that were within 2.5 km of each other, the ratios of NWS precipitation totals to ALERT precipitation totals ranged from 0.96 to 1.61. The median value was 1.18. Consequently, ALERT values were multiplied by 1.18 to adjust for the reduced precipitation totals associated with the tipping-bucket gauge [Heinemann *et al.*, 2002].

[9] Weather stations initially retained did not have more than 20% of days missing a precipitation total. This criterion was relaxed if the inclusion of a station with more than 20% missing data improved the spatial coverage of the network. Missing values at all stations were estimated using an inverse-distance weighting (IDW) scheme involving data from at least three nearby stations. Any station having data for the selected missing-data day was a potential predictor station. And in order to eliminate station clustering, the target minimum nearest-neighbor distances for stations in upland areas (i.e. $\geq 1,500$ m a.s.l.) and lowland areas (i.e. $< 1,500$ m a.s.l.) were 15 km and 30 km, respectively. The distance thresholds were chosen for the following reasons: a typical ridge to valley distance is approximately 15 km and Skirvin *et al.* [2003] found precipitation totals in southeastern Arizona to be approximately independent from one

another at distances of approximately 30 km. The final weather-station network was comprised of 115 stations exhibiting a random point pattern, with over 60% of the stations being NWS stations. Only 2% of the daily precipitation totals needed to be estimated, and only one station was originally missing more than 20% of its daily values.

[10] The other necessary dataset was a digital elevation model (DEM) with a spatial resolution of 30 m. The DEM was needed to determine the topographic settings of all the weather stations. The DEM – which is part of the National Elevation Dataset – was acquired from the United States Geological Survey.

3. Methods

[11] Multiple linear regression (MLR) modeling was used to reveal spatial anomalies in precipitation. MLR is an ideal technique for precipitation-anomaly detection: topography can be used a predictor and the resulting residuals – which are normally distributed – represent the amount of precipitation that is related more to geographic position than to local topographic characteristics.

[12] The predictands of the MLR models were total precipitation and frequency of heavy-precipitation days. Heavy-precipitation days were defined as days receiving at least 20 mm of precipitation. Heavy-precipitation-day frequency complements total precipitation, because it is less impacted by a small number of extreme precipitation events.

[13] Elevation, slope, and relief were the principal predictor variables. Elevation and slope values were obtained for 2,500 m, 5,000 m, 10,000 m, and 20,000 m circular neighborhoods centered on each weather station. Relief was calculated by subtracting the minimum elevation within each neighborhood from the spot elevation of the weather station. Spot elevations were provided in the station metadata. As a result, there were a total of 13 potential predictor variables (i.e. five elevation variables, four slope variables, and four relief variables).

[14] The modeling procedure involved predictor-variable selection and the creation of multiple MLR models. Principal components analysis (PCA) was employed to ensure that only independent variables were used in the modeling [see Kachigan, 1991]. Components with eigenvalues ≥ 1 were extracted and orthogonally rotated (i.e. VARIMAX) [e.g., Diem and Comrie, 2002]. A separate model was created for each combination of predictor variables, provided that no more than one predictor variable loaded highly on a single component. The MLR model that explained the most variance was selected to produce the precipitation anomalies.

[15] Residuals from the MLR models represented topographically-corrected precipitation values during the mon-

Table 1. Characteristics of MLR Models for Total Precipitation (TP) and Frequency of Heavy Precipitation Days (HPD)^a

Model	r^2	Predictor Variables and Y-Intercept
TP	0.75	E_{spot} (0.723), S_{10000} (22.424), R_{2500} (-0.894), Y-intercept (173.934)
HPD	0.58	E_{spot} (0.008), S_{10000} (0.384), R_{2500} (-0.007), Y-intercept (1.919)

^aBoth models had F-statistics with p-values less than 0.001, and all predictor variables had p-values less than 0.001. The predictor variables are as follows: E_{spot} is spot elevation; S_{10000} is mean slope of terrain within 10,000 m of station; and R_{2500} is maximum relief out to 2,500 m of station. Elevation and relief values were in meters, while the slope values were in degrees. Raw coefficients for the predictor variables and Y-intercept are provided in parentheses.

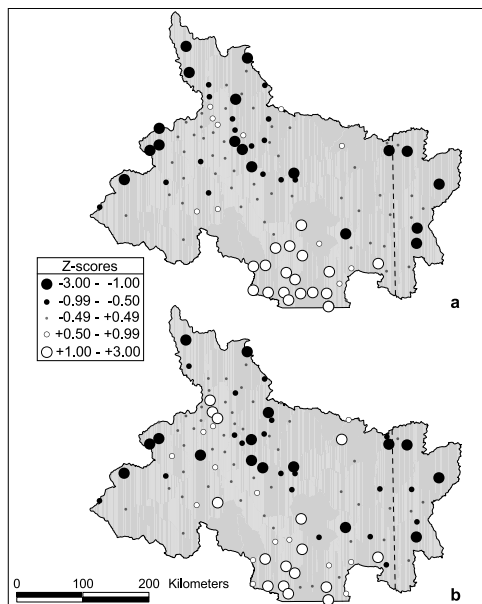


Figure 2. Standardized residuals from the multiple linear regression models for (a) total precipitation and (b) frequency of heavy-precipitation days. Dashed line is the Arizona/New Mexico border.

soon season. Each residual was converted to a Z-score, and absolute values of Z-scores greater than or equal to one represented strongly anomalous precipitation values.

4. Results and Discussion

[16] With total precipitation and frequency of heavy-precipitation days as the predictands, a total of 80 MLR models were created. Because the 13 potential predictor variables were reduced to three components (i.e. elevation, slope, and relief) that explained over 96% of the variance in the dataset, elevation, slope, and relief were the initial predictor variables in each of the models. There were 80 different combinations of elevation, slope, and relief. For both total precipitation and frequency of heavy-precipitation days, the following combination of variables produced the largest coefficient of determination (r^2) (Table 1): spot elevation, mean slope of terrain within 10,000 m of station, and maximum relief out to 2,500 m of station. The two models explained 75% and 58% of the variance in their respective predictands, thus a majority of the spatial variance in precipitation is controlled by local topography.

[17] Large positive residuals for both total precipitation and heavy-precipitation days are located almost entirely in south-central Arizona, which is hereafter also referred to as the intense monsoon zone (IMZ) (Figure 2). The IMZ is a zone of large underpredictions: the mean predicted seasonal precipitation total in the IMZ was 163 mm, whereas the mean observed total was 227 mm. Over-all south-central Arizona is relatively wet, since the mean observed seasonal precipitation total for the entire Gila River basin was 153 mm. *Michaud et al.* [1995] also found a zone of large positive residuals in south-central Arizona along with moderate positive residuals throughout most of the southern

half of Arizona. This present study has found the IMZ to be more concentrated in south-central Arizona. Although the IMZ's western boundary in southwestern Arizona is difficult to determine due to a lack of weather stations, the IMZ extends eastward to the Chiricahua Mountains and northward to the Santa Catalina Mountains (Figure 1). An additional positive-anomaly zone exists in the Bradshaw Mountains in the northwestern portion of the basin (Figure 2b); however, this zone is only comprised of three stations and it only exists for heavy-precipitation days.

[18] Large negative residuals for both total precipitation and heavy-precipitation days are scattered throughout the northern portion of the basin. No portion of the basin contains a majority of the large negative residuals. Therefore, there is not a negative-residual counterpart to the IMZ.

[19] Intense monsoonal activity associated with the SMO – which as noted earlier is the center of action for the Mexican monsoon – essentially extends into south-central and southeastern Arizona but not into New Mexico. With moisture provided by the Gulf of California via upslope flow, moist air parcels over the SMO should move northwestward into southern Arizona [*Mullen et al.*, 1998]. In addition, lower-tropospheric flow should transport water from the Gulf of California directly to the south-central portion of the Gila River basin [e.g., *Douglas and Li*, 1996; *Stensrud et al.*, 1997; *Mullen et al.*, 1998; *Anderson et al.*, 2000; *Berberly*, 2001]. Much of the precipitation in the IMZ may be tied to strong surges of moisture from the Gulf of California (i.e. gulf surges), for *Higgins et al.* [2004] showed how positive precipitation anomalies move from the SMO on the date of surge onset northward into southern Arizona several days later.

5. Conclusions

[20] This paper presented an examination of topographically-corrected summer precipitation values for 115 stations within the Gila River basin. MLR models with topographic variables as predictors were produced, and the models explained at least 75% and 58% of the variance in total precipitation and frequency of heavy-precipitation days, respectively. Since the residuals were approximately normally distributed, clusters of Z-scores ≥ 1 were classified as relatively intense monsoonal zones.

[21] An intense monsoonal zone encompassed south-central Arizona. The zone also probably included most of southeastern Arizona. It was concluded that this zone represented a direct northward propagation of the Mexican monsoon.

[22] Future work is required to verify both the existence and causes of anomalous precipitation values in the Gila River basin. Spatially continuous lightning-flash data should be a viable proxy for precipitation magnitude, thus lightning data could be examined for significant spatial anomalies in the basin. In addition, the role of moisture transport needs to be assessed, such as through a spatial examination of dew-point temperatures.

References

- Anderson, B. T., J. O. Roads, S.-C. Chen, and H.-M. H. Juang (2000), Regional simulation of the low-level monsoon winds over the Gulf of California and southwestern United States, *J. Geophys. Res.*, 105(D14), 17,955–17,969.

- Balling, R. C., and S. W. Brazel (1987), Diurnal variations in Arizona monsoon precipitation frequencies, *Mon. Weather Rev.*, *115*, 342–346.
- Berbery, E. H. (2001), Mesoscale moisture analysis of the North American monsoon, *J. Clim.*, *14*, 121–137.
- Comrie, A. C., and B. Broyles (2002), Variability and spatial modeling of fine-scale precipitation data for the Sonoran Desert of south-west Arizona, *J. Arid Environ.*, *50*, 573–592.
- Comrie, A. C., and E. C. Glenn (1998), Principal components-based regionalization of precipitation regimes across the southwest United States and northern Mexico, with an application to monsoon precipitation variability, *Clim. Res.*, *10*, 201–215.
- Diem, J. E., and A. C. Comrie (2002), Predictive mapping of air pollution involving sparse spatial observations, *Environ. Pollut.*, *119*, 99–117.
- Douglas, M. W., and S. Li (1996), Diurnal variation of the lower-tropospheric flow over the Arizona low desert from SWAMP-1993 observations, *Mon. Weather Rev.*, *124*, 1211–1224.
- Douglas, M. W., R. A. Maddox, and S. Reyes (1993), The Mexican monsoon, *J. Clim.*, *6*, 1665–1677.
- Heinemann, A. B., G. Hoogenboom, and B. Chojnicki (2002), The impact of potential errors in rainfall observation on the simulation of crop growth, development and yield, *Ecol. Modell.*, *157*, 1–21.
- Higgins, R. W., Y. Chen, and A. V. Douglas (1999), Interannual variability of the North American warm season precipitation regime, *J. Clim.*, *12*, 653–680.
- Higgins, R. W., W. Shi, and Y. Chen (2004), Relationships between Gulf of California moisture surges and precipitation in the southwestern United States, *J. Clim.*, *17*, 2983–2997.
- Kachigan, S. K. (1991), *Multivariate Statistical Analysis: A Conceptual Introduction*, Radius Press, New York.
- Michaud, J. D., B. A. Auvine, and O. C. Penalba (1995), Spatial and elevational variations of summer rainfall in the southwestern United States, *J. Appl. Meteorol.*, *34*, 2689–2703.
- Mitchell, D. L., D. Ivanova, R. Rabin, T. Brown, and K. Redmond (2002), Gulf of California sea surface temperatures and the North American monsoon: Mechanistic implications from observations, *J. Clim.*, *15*, 2261–2281.
- Mullen, S. L., J. T. Schmitz, and N. O. Renno (1998), Intraseasonal variability of the summer monsoon over southeast Arizona, *Mon. Weather Rev.*, *126*, 3016–3035.
- Rowson, D. R., and S. J. Colucci (1992), Synoptic climatology of thermal low-pressure systems over south-western North America, *Int. J. Climatol.*, *12*, 529–545.
- Saleeby, S. M., and W. R. Cotton (2004), Simulations of the North American monsoon system. part I: Model analysis of the 1993 monsoon season, *J. Clim.*, *17*, 1997–2018.
- Skirvin, S. M., S. E. Marsh, M. P. McClaran, and D. M. Meko (2003), Climate spatial variability and data resolution in a semi-arid watershed, south-eastern Arizona, *J. Arid Environ.*, *54*, 667–686.
- Stensrud, D. J., R. L. Gall, S. L. Mullen, and K. W. Howard (1995), Model climatology of the Mexican monsoon, *J. Clim.*, *8*, 1775–1794.
- Stensrud, D. J., R. L. Gall, and M. K. Nordquist (1997), Surges over the Gulf of California during the Mexican monsoon, *Mon. Weather Rev.*, *125*, 417–437.
- Watson, A. I., R. E. Lopez, and R. L. Holle (1994), Diurnal cloud-to-ground lightning patterns in Arizona during the southwest monsoon, *Mon. Weather Rev.*, *122*, 1716–1725.
- Wright, W. E., A. Long, A. C. Comrie, S. W. Leavitt, T. Cavazos, and C. Eastoe (2001), Monsoonal moisture sources revealed using temperature, precipitation, and precipitation stable isotope timeseries, *Geophys. Res. Lett.*, *28*, 787–790.

J. E. Diem, Department of Anthropology and Geography, Georgia State University, Atlanta, GA 30303-3081, USA. (gegjed@langate.gsu.edu)